Formation of carcinogens indoors by surface-mediated reactions of nicotine with nitrous acid, leading to potential *thirdhand smoke* hazards

Mohamad Sleiman[a], Lara A. Gundel[a], James F. Pankow[b], Peyton Jacob III[c], Brett C. Singer[a], and Hugo Destaillats[a,d,1]

[a]Indoor Environment Department, Lawrence Berkeley National Laboratory, 1 Cyclotron Road, MS 70-108B, Berkeley, CA 94720; [b]Department of Chemistry, Portland State University, Portland, OR 97201; [c]Departments of Medicine and Psychiatry, University of California San Francisco, CA 94143; and [d]School of Sustainable Engineering and the Built Environment, Arizona State University, Tempe, AZ 85287

Edited by Barbara J. Finlayson-Pitts, University of California, Irvine, Irvine, CA, and approved January 6, 2010 (received for review November 7, 2009)

This study shows that residual nicotine from tobacco smoke sorbed to indoor surfaces reacts with ambient nitrous acid (HONO) to form carcinogenic tobacco-specific nitrosamines (TSNAs). Substantial levels of TSNAs were measured on surfaces inside a smoker's vehicle. Laboratory experiments using cellulose as a model indoor material yielded a >10-fold increase of surface-bound TSNAs when sorbed secondhand smoke was exposed to 60 ppbv HONO for 3 hours. In both cases we identified 1-(*N*-methyl-*N*-nitrosamino)-1-(3-pyridinyl)-4-butanal, a TSNA absent in freshly emitted tobacco smoke, as the major product. The potent carcinogens 4-(methylnitrosamino)-1-(3-pyridinyl)-1-butanone and *N*-nitroso nornicotine were also detected. Time-course measurements revealed fast TSNA formation, with up to 0.4% conversion of nicotine. Given the rapid sorption and persistence of high levels of nicotine on indoor surfaces—including clothing and human skin—this recently identified process represents an unappreciated health hazard through dermal exposure, dust inhalation, and ingestion. These findings raise concerns about exposures to the tobacco smoke residue that has been recently dubbed "thirdhand smoke." Our work highlights the importance of reactions at indoor interfaces, particularly those involving amines and NO_x/HONO cycling, with potential health impacts.

exposure | indoor environment | nitrosamine | nitrogen oxides | heterogeneous chemistry

Tobacco use causes 20% of cancer deaths worldwide. The International Agency for Research on Cancer predicts 10 million tobacco-related deaths annually by 2020, of which 70% will occur in the developing world (1). Over the past decade, the United States (US) and other countries have successfully reduced the exposure of nonsmokers to *secondhand smoke* (SHS, smoke inhaled unintentionally) in public spaces and the workplace. Nevertheless, the US Surgeon General 2006 report warned that progress has been slower in the protection of young children, for whom the most important exposure setting is the home (2). Whereas direct inhalation of SHS is an exposure pathway of concern, nonsmokers, especially infants, are at risk through contact with surfaces and dust contaminated with residual smoke gases and particles (3). This type of lingering residue of tobacco smoke has recently been called *thirdhand smoke* (THS) (4). Whereas desorption from indoor surfaces to air has been recognized for some time as a source of subsequent exposure (5–7), the potential for chemical transformation has been examined only recently (8). Reactions of atmospheric species [O_3, nitrous acid (HONO), NO_x] with residual smoke on surfaces (furniture, walls, skin, clothing) have been overlooked as a source of long-term exposure to harmful pollutants.

This study is an exploration of the in situ reaction of nicotine sorbed to indoor surfaces with HONO to form tobacco-specific nitrosamines (TSNAs). These chemicals are among the most broadly acting and potent carcinogens present in unburned tobacco and tobacco smoke (9, 10). Nicotine, their precursor, is the most abundant organic compound emitted during smoking (up to 8 mg per cigarette). It deposits almost entirely on indoor surfaces and persists for weeks to months (6, 7). HONO is often present in indoor environments at higher levels than outdoors. Typical indoor levels are 5–15 ppbv, with [HONO]/[NO_2] ratios ~0.15 to 0.4 (vs. ~0.03 outdoors). Indoor levels up to 100 ppbv have been reported (11–13). The main indoor sources of HONO are direct emissions from unvented combustion appliances (14, 15), smoking (16), and surface conversion of NO_2 and NO (17–22). Heterogeneous formation of HONO also occurs inside automobiles, leading to [HONO] up to 30 ppbv and [HONO]/[NO_2] ~ 0.4 in polluted urban areas (23). Pitts et al. (24) first described the atmospheric production of *N*-nitrosamines by reactions of nitrogen oxides and HONO with amines. *N*-nitrosamines were found to be unstable in sunlight, rendering the reaction unimportant in outdoor daytime conditions. However, this process can be relevant indoors where *N*-nitrosamines and HONO are less vulnerable to photochemical decomposition.

Results and Discussion

Indoor Nitrosation of Nicotine. Three main TSNAs are formed in the reaction of sorbed nicotine and gaseous HONO: 1-(*N*-methyl-*N*-nitrosamino)-1-(3-pyridinyl)-4-butanal) (NNA), 4-(methylnitrosamino)-1-(3-pyridinyl)-1-butanone (NNK), and *N*-nitroso nornicotine (NNN). In field measurements, we detected TSNAs on interior surfaces of a truck driven by a heavy smoker. Fig. 1*A* shows the concentrations of surface-bound TSNAs on the stainless-steel glove compartment (Truck-A) and on cellulose substrates attached next to it (Truck-B), for 3 days in which smoking occurred in the vehicle. In both samples, two TSNAs, NNA and NNK, were detected at appreciable levels (1–5 ng cm^{-2}).

Whereas NNK is known to be present in tobacco smoke particles, NNA has not been reported previously, probably because of its reactivity and instability at high temperatures during tobacco pyrolysis (9). A mechanism to explain the in situ formation of surface-bound TSNAs measured in this study is proposed below. The predominance of NNA is consistent with results by Hecht et al. (25), who showed that NNA was the main product of nicotine nitrosation in acidic $NaNO_2$ solution (pH 5.4–5.9). We hypothesize that similar processes occur on indoor surfaces exposed to ambient HONO.

Author contributions: M.S., L.A.G., J.F.P., P.J., B.C.S., and H.D. designed research; M.S., L.A.G., and H.D. performed research; P.J. contributed new reagents/analytic tools; M.S., L.A.G., J.F.P., P.J., B.C.S., and H.D. analyzed data; and M.S., L.A.G., J.F.P., P.J., B.C.S., and H.D. wrote the paper.

The authors declare no conflict of interest.

This article is a PNAS Direct Submission.

[1]To whom correspondence should be addressed. E-mail: HDestaillats@lbl.gov.

This article contains supporting information online at www.pnas.org/cgi/content/full/0912820107/DCSupplemental.

Laboratory experiments using cellulose as a model surface were carried out to test this hypothesis. Cellulose substrates were exposed to vaporized nicotine in a tubular-flow reactor, obtaining a loading of 9.1 $\mu g\,cm^{-2}$, before equilibration with HONO (65 ppbv). The resulting production of surface-bound NNA and NNK (with [NNA]/[NNK] = 7) confirms that both TSNAs derive from nicotine (sample Nic, Fig. 1*A*). NNN was detected at levels too low for accurate quantification. Similar results were found when cellulose substrates containing sorbed tobacco smoke (sorbed SHS) were exposed to HONO for 3 hours. In the resulting sample (THS), TSNA surface concentrations increased at least 10-fold. Furthermore, in all samples exposed to HONO (THS, Nic, Truck-A, Truck-B), the steady-state ratio of total TSNA concentrations to surface nicotine expressed in mass units

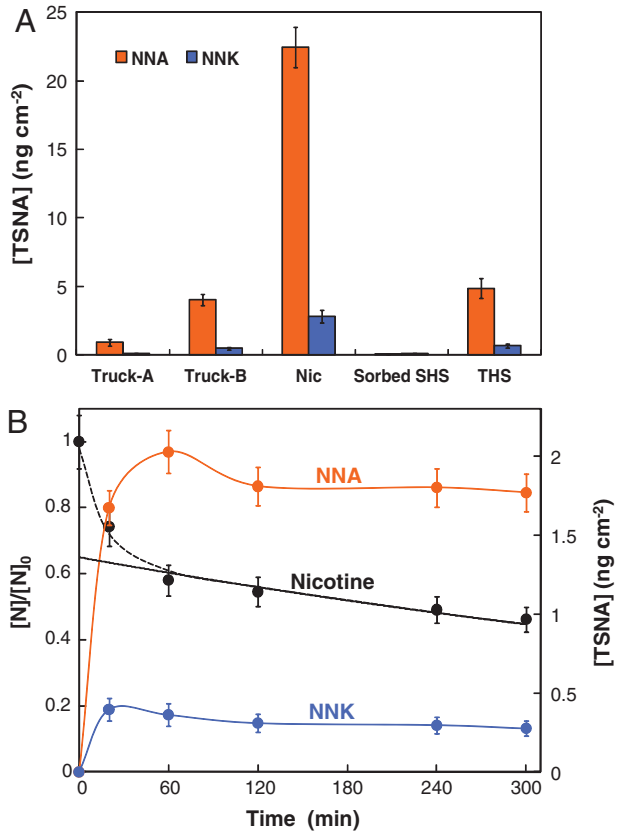

Fig. 1. Formation of TSNAs from nitrosation of nicotine. (*A*) Surface concentrations of NNA and NNK. In field experiments, sample Truck-A was obtained inside the cabin of a smoker's truck by wiping the stainless-steel surface of the door of the glove compartment, on which 0.6 $\mu g\,cm^{-2}$ of nicotine was present. Another sample (Truck-B) was collected on clean cellulose substrates that were attached to cabin surfaces for 3 days, over which 34 cigarettes were smoked. The cellulose surface sorbed nicotine passively (1.4 $\mu g\,cm^{-2}$) and also served as reaction medium for the formation of TSNAs. In lab experiments, cellulose substrates were exposed to nicotine vapor (9.1 $\mu g\,cm^{-2}$) and subsequently exposed to HONO (Nic). The same substrates were exposed to sidestream smoke in an environmental chamber, leading to loadings of 1.9 $\mu g\,cm^{-2}$ nicotine, with negligible levels of NNA and NNK (Sorbed SHS). After a 3-hour exposure of this sample to HONO, formation of NNA and NNK on the surface was observed (THS). (*B*) Time course of nicotine loss and production of NNA and NNK. Cellulose substrates were impregnated with nicotine with an initial surface concentration $[N]_0$ of 1.45 $\mu g\,cm^{-2}$ and subsequently exposed to $[HONO]_0 = 95$ ppbv in a tubular-flow reactor over different periods of time (relative humidity 45%). A biexponential model was fitted to the nicotine surface concentration profile to derive the contributions of desorption and chemical reaction processes. [TSNA] corresponds to the surface concentrations of NNA and NNK, and [N] represents the surface concentration of nicotine. Concentrations were determined by using the exposed geometric areas.

was about 1:250 (equivalent to 1:320 in mole units), corresponding to nicotine conversions of $\chi_{NNA} = [NNA]/[N] = 3.5 \times 10^{-3}$ and $\chi_{NNK} = [NNK]/[N] = 0.5 \times 10^{-3}$ (for concentrations expressed in mass units). In a separate experiment, a cellulose substrate loaded with similar nicotine levels was exposed to high levels of NO and NO_2 (290 and 560 ppbv, respectively), in the absence of gas-phase HONO. We observed formation of only trace amounts of NNA and NNK (close to the limit of detection) together with a slight decrease in NO_2 concentration, on the order of ~5 ppbv. These results are consistent with surface-mediated conversion to HONO and subsequent nitrosation of nicotine.

Fig. 1*B* shows time-concentration profiles for surface nicotine and TSNAs in laboratory experiments. Both NNA and NNK formed rapidly, reaching maximum concentrations within the first hour. Formation rates of TSNAs were $R_{NNA} = \partial[NNA]/\partial t = (8.4 \pm 0.6)10^{-2}$ ng cm^{-2} min^{-1} $(0.24 \pm 0.02\ \mu mol\,m^{-2}\,h^{-1})$ and $R_{NNK} = \partial[NNK]/\partial t = (2.0 \pm 0.4)10^{-2}$ ng cm^{-2} min^{-1} $(0.06 \pm 0.01\ \mu mol\,m^{-2}\,h^{-1})$, respectively, estimated from the initial slope ($t < 20$ min) in Fig. 1*B*, assuming that the initial decomposition rate was negligible. The shapes of the NNA and NNK curves suggest that freshly formed TSNAs are protected from attack by HONO by chemical and/or physical processes (e.g., diffusion into the cellulosic media). A biexponential model was fitted to the surface nicotine concentration profile to estimate contributions from chemical reaction and desorption. The fitted rate constant for nicotine reaction of $k_N = 1.25 \times 10^{-3}$ min^{-1} corresponds to nicotine reactive loss rates in the range $R_N = -\partial[N]_S/\partial t = 1.5 - 1.1$ ng cm^{-2} min^{-1} $(5.5 - 4.1\ \mu mol\,m^{-2}\,h^{-1})$. The nicotine reaction rate was almost identical to the HONO reactive uptake rate ($R_{HONO} = 5.5\ \mu mol\,m^{-2}\,h^{-1}$; see *SI Text*), corresponding to a HONO mass transfer coefficient of 2.1 $m\,h^{-1}$. This value is the same order of magnitude as the boundary-layer mass transfer coefficient in buildings (26, 27), suggesting that reaction with nicotine may be a strong sink for HONO indoors.

Assuming first-order reaction kinetics, the relative yield (ϕ_{TSNA}) of TSNAs can be estimated from initial reaction rates as

$$\phi_{TSNA} = \frac{R_{NNA} + R_{NNK}}{R_N} * 100. \quad [1]$$

TSNA yields were $\phi_{TSNA} = 6.7$–9.1% by mass (5.4–7.3% by mole). These relatively high yields call attention to the importance of this reaction as a source of tobacco carcinogens on indoor surfaces.

Additional tests were carried out to assess the stability of TSNAs in the presence of HONO. Cellulose substrates were spiked with TSNAs dissolved in water-methanol (95/5) and were subsequently exposed to HONO (60 ppbv) under the same conditions as reported above. Slightly more than 50% of the initial NNA was lost in 2 hours, but NNN and NNK were more stable, with just 20–30% loss over the same period. These findings are in agreement with results shown in Fig. 1*B* and suggest that after their fast initial formation TSNAs undergo partial degradation by HONO, to reach steady-state concentrations.

Reaction Mechanism and Products. Fig. 2*A* presents a schematic representation of the main physical-chemical processes involved in the surface-mediated nitrosation of nicotine. In Fig. 2*B*, we propose a mechanism for heterogeneous TSNA formation consistent with the products observed in our experiments. The main reactive species is assumed to be NO^+, which removes one electron from the pyrrolidine nitrogen of nicotine to form an unstable cation intermediate. A second NO^+ abstracts a hydrogen atom from one of the three α-carbon atoms (a, b, and c) yielding an iminium ion. Successive reaction of iminium with water and HONO generates the corresponding TSNA. The prevalence of NNA can be

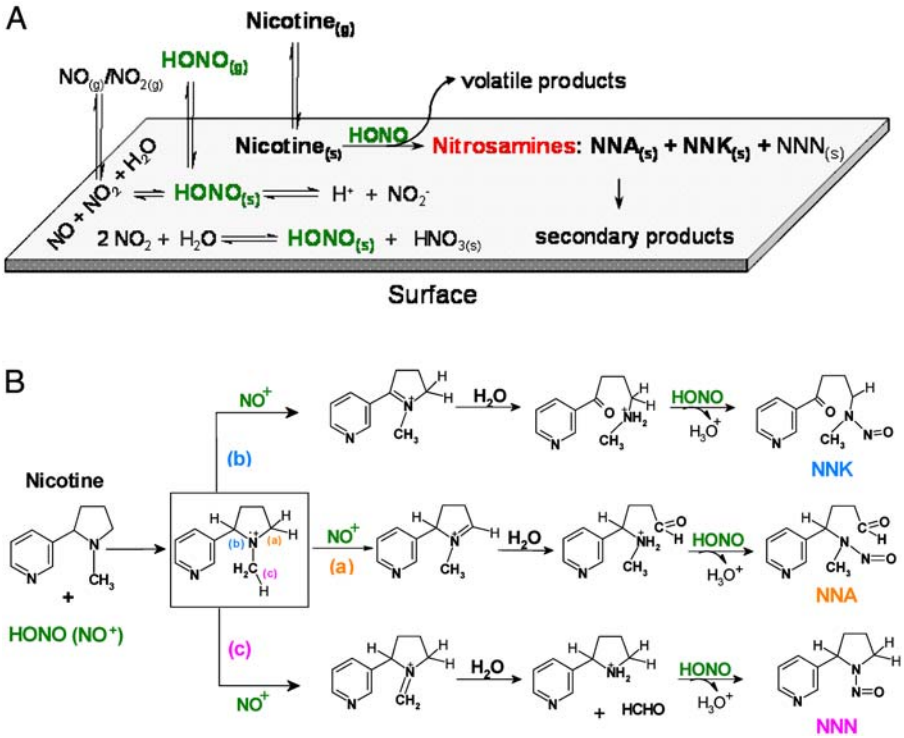

Fig. 2. Physical-chemical processes involved in the formation of TSNAs. (*A*) Illustration of surface-mediated nitrosation of nicotine. $HONO_{(s)}$ can be formed through three pathways: (*i*) direct adsorption of $HONO_{(g)}$, (*ii*) heterogeneous disproportionation of NO_2, and (*iii*) surface-catalyzed reaction between NO and NO_2. $HONO_{(s)}$ reacts with nicotine generating NNA and NNK. NNN was also produced with lower yields. Secondary products are listed in Table 1. (*B*) Proposed mechanism for the formation of TSNAs. The first step involves the electrophilic attack of NO^+ on nicotine, leading to the formation of the unstable cationic intermediate shown in the box. The second step is initiated with abstraction of a hydrogen atom to form an iminium cation, which is then hydrolyzed by sorbed water molecules. Finally, HONO nitrosates the secondary amines to form NNA, NNK, and NNN.

attributed to a regioselective abstraction of a 5′ hydrogen atom (position a), in analogy to chemical and biological oxidation of nicotine, in which that position is most susceptible to attack by electrophilic species (28). An alternative mechanism, similar to that proposed by Hecht et al. (25) is presented in *SI Text* and leads to identical products. The acidity of the aqueous surface layer [pH ~5–6 in the absence of HONO (29)] plays a key role by inducing the formation of NO^+ and affecting regioselectivity. In addition to TSNAs, we observed the formation of secondary products in the gas phase and on surfaces, as summarized in Table 1. These included TSNA degradation products such as *N*-nitrosopyrrolidine (**2**, a carcinogenic volatile nitrosamine), a surface-bound product formed through *C*-nitrosation of NNK (**5**), and a stable pyrazole compound (**7**), resulting from NNA decomposition. For the latter, we describe two possible reaction pathways for its formation from NNA in *SI Text* (25, 30). The pyrazole (**7**) was formed with a higher yield than the total TSNAs, and it has not been reported in freshly emitted SHS. Therefore, it could be used as a tracer for the THS products formed by HONO-nicotine chemistry.

Implications for Indoor Exposures. The in situ formation of TSNAs presents a specific concern about the hazards of THS. NNK is a strong carcinogen, with reported cancer potency of 49 $kg\,mg^{-1}\,d^{-1}$ (10). It has been shown to induce mutations, DNA strand breaks, and oxidative damage under sunlight, in the absence of metabolic activation (31). NNA carcinogenicity has not been reported, but its mutagenic activity is similar to that of NNN (32). Our findings warrant further investigation of the NNA toxicity and human intake. Monitoring of its likely metabolite 4-(methylnitrosamino)-4-(3-pyridyl)-1-butanol (iso-NNAL) could be used to assess nonsmokers' intake of NNA, by analogy to the current use as a biomarker of 4-(methylnitrosamino)-1-(3-pyridyl)-1-butanol (NNAL), formed by metabolic reduction of NNK (33). The precursor to iso-NNAL, NNA, has not been identified in tobacco (34, 35).

There are several potentially important exposure routes through which surface-formed TSNAs may enter the body. Direct inhalation of gas-phase TSNAs is likely negligible, given their very low vapor pressures [in pressure units of mm Hg, $\mathrm{Log}_{10}P^0_{\mathrm{NNA}} = -6.67$ and $\mathrm{Log}_{10}P^0_{\mathrm{NNK}} = -6.72$ (36)]. Instead, dermal contact with surfaces contaminated by TSNAs (skin, clothing, and furnishings), as well as inhalation and ingestion of TSNA-loaded dust, are likely the main exposure pathways. On the basis of the framework developed by Weschler and Nazaroff (37) to assess indoor exposures to semivolatile organic compounds, we estimated the surface loading of nicotine (M_N) as

$$M_N = K_{\mathrm{oa}}\delta[\mathrm{N}]_g S_H, \qquad [2]$$

where K_{oa} is the octanol-air partition coefficient of nicotine ($\log K_{\mathrm{oa}} = 7.8$) (7), δ is the thickness of an organic film on the skin surface (using 10 nm as a conservative estimate), $[\mathrm{N}]_g$ is the gas-phase concentration of nicotine, and S_H is the exposed surface of the human skin [calculated as 20% of the total estimated human envelope surface, 2 m^2 (37)]. We predict nicotine levels on human skin to be 0.63–63 $\mu g\,m^{-2}$ ($M_N = 0.25$–25 μg), in equilibrium with gas-phase nicotine concentrations between 1 and 100 $\mu g\,m^{-3}$, corresponding to typical and high levels reported in homes and public places where smoking takes place, respectively (2). This is consistent with reported levels >80 $\mu g\,m^{-2}$ on the index fingers of smokers (an extreme-case scenario for skin levels) (3). In the presence of HONO, skin-bound nicotine could react to produce TSNAs at the concentrations shown in Table 2. Nicotine surface concentrations ranging from 5 to 100 $\mu g\,m^{-2}$ have been measured in dust, on surfaces inside vehicles

Table 1. Secondary products of nicotine heterogeneous nitrosation by HONO.

	Product no.	Product name	Product structure	*m/z*	Yield %*
Gas-phase products	1	Formaldehyde		N/A†	<0.05
	2	*N*-nitroso-pyrrolidine	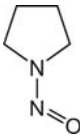	100, 70, 68	<0.05
	3	Methyl 3-pyridinecarboxylate (Methyl nicotinate)	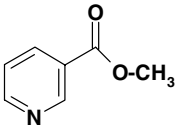	137, 106, 78	<0.05
	4	N-methylNicotinamide	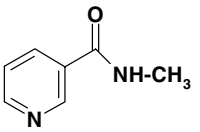	136, 106, 78	0.1
Cellulose-sorbed species	5	4-(N-methyl-N-nitrosamino)-2-oxi-mino-1-(3-pyridyl)-1-butanone	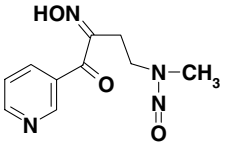	219, 106, 130, 165, 78	<0.05
	6	1-methyl-5-pyridin-3-yl-pyrrolidin-2-one (Cotinine)	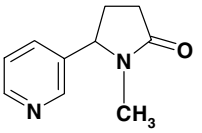	176, 118, 98	0.3
	7	1-methyl-5-(3 pyridinyl) pyrazole	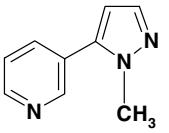	159, 158, 130, 118, 104, 78	0.8

*Yields were determined on the basis of the ratio of peak areas of each product over nicotine.
†Formaldehyde was determined by dinitrophenylhydrazine derivatization and HPLC analysis with UV detection.

(dashboards) (38), and in households of smokers (tables and bed frames) (3) (Table 2). Cotton, a material commonly used in clothing, upholstery, and draperies, sorbs substantial amounts of nicotine, up to 100 $mg\,m^{-2}$, with ~1 $mg\,m^{-2}$ remaining after one week of desorption in a clean air flow (8). The levels of TSNAs formed in each of those surfaces under typical HONO levels, also presented in Table 2, were estimated as $[NNA] = [N] * \chi_{NNA}$ and $[NNK] = [N] * \chi_{NNK}$. TSNA-laden particles abraded from clothes and skin may enter the breathing zone as part of the personal reactive cloud, thus contributing to additional intake through inhalation (39–41).

Given the low volatility of TSNAs and the high levels of nicotine typically found in environments contaminated with tobacco smoke, these carcinogens can persist indoors (42) and on the human envelope. Because of their frequent contact with surfaces and dust, infants and children are particularly at risk. At approximately 0.05–0.25 $g\,day^{-1}$, the dust ingestion rate in infants is estimated to be more than twice that of adults (3). Moreover, considering that infants have a higher respiration rate (by a factor of 3–8) and a lower body weight than adults (by a factor of 10–20), low doses of TSNAs such as those reported in Table 2 may represent a potential long-term health hazard.

Various mitigation and remediation approaches can be considered to limit the impact of these carcinogenic pollutants indoors. Implementation of 100% smoke-free environments in public places and self-restrictions in residences and automobiles are the most effective tobacco control measures, through elimination of the primary pollution source. In buildings where substantial smoking has occurred, replacing nicotine-laden furnishings, carpets, and wallboard can significantly reduce exposures to THS hazards. More research is needed on the identification and characterization of specific biomarkers to assess human intake of NNA and other THS pollutants and to better understand their health implications. Research is also needed to explore other reactions of atmospheric species at indoor interfaces that may impact human health (43).

Materials and Methods

Tubular-Flow Reactor, Ancillary Laboratory Setup, and Methodology. Laboratory experiments were performed by using a glass tubular-flow reactor (length: 33 cm; diameter: 1 cm; flow rate: 0.5 L min^{-1}). Upstream, "zero" grade air was humidified to 45% relative humidity by passage through an impinger before entering the reactor containing two identical cellulose substrates (23 cm × 1 cm × 3 mm, Whatman 3030-153). HONO was generated continuously, by following the method described by Taira and Kanda (44). Two syringe pumps delivered H_2SO_4 (0.022 M) and $NaNO_2$ (0.001 M) into a Teflon reaction vessel, where the evolved HONO vapor was entrained in the air flow to the reactor. Downstream of the reactor, the flow could be split into three streams to determine (*a*) HONO/NO/NO_2 by using a NO_x analyzer, (*b*) HONO by ion chromatography, and (*c*) volatile products. *SI Text* illustrates the experimental setup.

Adsorption of nicotine on cellulose substrates. Nicotine vapor was generated upstream of the reactor by circulating a dry air stream over

Table 2. Nicotine and TSNA concentrations on households, vehicle surfaces, and human skin. Calculations were based on the nicotine conversions to NNA (0.35%) and NNK (0.05%), expressed in mass units

Surface		[N] ($\mu g\,m^{-2}$)	[NNA] ($ng\,m^{-2}$)	[NNK] ($ng\,m^{-2}$)
Households	Furniture*	11–73	37–256	5.3–36.5
	Dust*	0.89–4.43	3–15	0.44–2.2
Vehicles	Dashboard*	5.0–8.6	17–30	2.5–4.3
	Dust*	11.6–19.5	41–68	6.1–9.7
Skin and clothing	Skin*	>80	>280	>40
	Skin†	0.63–63	2.2–220	0.31–31
	Cotton‡	1000	3500	500

*Values estimated from Matt et al. (3).
†Estimates based on Weschler and Nazaroff (37).
‡Determined based on Destaillats et al. (8).

a beaker containing liquid nicotine (>99%; Aldrich) placed in a sealed vessel at 23 °C. The nicotine vapor supply concentration was 153 ± 17 nmol L^{-1} (8). The nicotine-containing air stream was mixed with humid air to reach relative humidity of 45% and directed to the reactor during the initial adsorption phase of each experiment (10 min to 2 hours). At the end of this period, one substrate was removed to determine the initial nicotine loading, and the nicotine source was disconnected prior to introduction of HONO (or NO/NO_2).

Reaction of nicotine with HONO and with a NO/NO_2 mixture. Once nicotine adsorption was completed, HONO was introduced into the reactor. In a few experiments we evaluated the reaction of nicotine with nitrogen oxides (*in lieu* of HONO) by directly introducing a diluted mixture of NO and NO_2 (290 and 560 ppb, respectively) into the reactor airstream from a Tedlar bag.

Monitoring of HONO, NO, and NO_2. The concentration of HONO was measured in real time downstream of the reactor by using a NO_x analyzer (API Model 200 E; TELEDYNE instruments). Gas-phase HONO concentrations were recorded as NO_2 concentration. The absence of NO_2 in the system was verified by scrubbing HONO with a $CaCO_3$-impregnated quartz filter upstream of the NO_x monitor. HONO was also trapped in an impinger filled with a NaOH aqueous solution (pH 10, volume = 5 mL) and analyzed by ion chromatography (Dionex ICS-2000). When NO and NO_2 were injected, their concentrations were followed by using the NO_x analyzer.

Analysis of gas-phase species. Nicotine and volatile products formed during its reaction with HONO were collected by using (*i*) an impinger filled with methanol (5 mL) in an ice bath, analyzed by gas chromatography–ion trap–tandem mass spectrometry (GC-IT-MS/MS); (*ii*) dual sorbent glass tubes containing Tenax-TA and Carbosieve SIII, followed by analysis on an Agilent 6890 GC equipped with an automated thermal desorption inlet with autosampler (Gerstel 3A) and an Agilent 5973 mass selective detector operated in electron impact mode, under operational parameters reported previously (8); and (*iii*) dinitrophenylhydrazine-coated silica cartridges (Waters Sep-Pak Xposure, WAT047205) to collect volatile aldehydes, followed by extraction using acetonitrile (2 mL) and HPLC-UV analysis (Agilent 1200 series).

Surface products extraction and analysis. Nicotine and its reaction products were extracted from cellulose surfaces with methanol. Each cellulose substrate was cut into two halves and weighed. Each half was transferred to a 40-mL amber flask, where 5 mL of methanol spiked with quinoline (internal standard) were added. Next, the flasks were stirred for 25 min and slurries centrifuged for 20 min at 10,000 rpm to separate the supernatant from suspended paper particles. A 1-mL aliquot was transferred to an amber vial for GC-IT-MS/MS analysis, whereas the remaining supernatant was archived. Recoveries of nicotine, NNA, and NNK ranged from 90 to 115%. The same procedure was followed for extraction of the passively exposed cellulose samplers and wipe samples collected in field measurements.

Preparation of SHS-Coated Cellulose Samples and SHS Characterization. SHS-coated cellulose substrates were collected in an Lawrence Berkeley National Laboratory (LBNL) room-sized 18-m^3 environmental chamber with low background concentrations of airborne contaminants. SHS was generated in the chamber by using a smoking machine (ADL/II smoking system; Arthur D. Little, Inc.). Nine cigarettes of a major US brand were smoked at equal intervals over a 3-hour period. The main experimental conditions for the chamber test are summarized in *SI Text*. Three different types of samples were collected.

Sorbed SHS (passive sampling). Passive samples were collected on cellulose substrates placed on a horizontal surface, to simulate deposition of SHS pollutants on indoor surfaces. Rectangular cellulose strips (Whatman cat. no. 3030-153, 23 cm × 1 cm × 3 mm) were placed on a table covered with aluminum foil at a distance of ~1 m from the smoking machine.

Particle-bound TSNAs (active sampling). Active sampling of airborne SHS particles was carried out continuously during the 3-hour period by using two Teflon-coated glass filters (Pall TCGF, 90 mm diameter) in series, at 100 L min^{-1}. The filters were preceded by a cyclone (URG Corporation) to remove any particles larger than 2.5 μm diameter. After collection, the TCGF filters were individually wrapped in clean aluminum foil envelopes, placed in clean plastic containers, and stored in the freezer at −30 °C prior to extraction and analysis.

Gas-phase nicotine. Gas-phase nicotine was actively sampled by using Tenax-TA sorbent glass tubes. Tenax tubes were analyzed as described previously (8), by using an HP 5890 GC equipped with an ATD400 thermal desorption inlet (Perkin Elmer) and a nitrogen and phosphorous-sensitive detector (DET Engineering).

Field Sampling. Two samples were collected inside the passenger compartment of an old (1966) light duty pickup truck in which the driver routinely smoked while commuting. Sample Truck-A, representing the background loading of nicotine and TSNAs, was collected by wiping an area (12 cm × 15 cm) on the outside of the metal door of the glove compartment with clean laboratory tissue that had been wetted with 5 mL spectroscopic grade ethanol. The tissue was transferred to a clean glass vial for storage in a freezer (−30 °C) prior to analysis. Sample Truck-B was collected on a cellulose substrate (identical to those used in lab experiments) with exposed area of 12 cm × 15 cm, with no direct exposure to sunlight. The cellulose substrate was secured in a frame made from clean aluminum foil and mounted over the area that had been wiped to generate sample Truck-A. The cellulose was exposed to SHS over the next 3 days during which the driver smoked 34 cigarettes inside the vehicle.

TSNA Analysis. ***GC-IT-MS/MS.*** Extracts were analyzed by GC-IT-MS/MS by using a Varian 3800 gas chromatograph (Varian Chromatography Systems) equipped with a CP8400 autosampler and ion trap mass detector Varian 2000. Methanol extracts were injected directly into the GC operating in splitless mode at 200 °C. Representative GC-IT-MS/MS chromatograms are shown in *SI Text*. Nicotine and TSNAs were separated on a 30 m VF-5 MS, low bleed column. The mass spectrometer was operated in the electron ionization mode at 70 eV in the mass range 50 to 350 *m/z*. For MS/MS, precursor ions of NNN (*m/z* 147), NNA (*m/z* 148), and NNK (*m/z* 177) were used, whereas fragment ions selected for quantification were 105, 130, and 132 for NNN, 148 for NNA, and 146, 149, and 159 for NNK. Quinoline was used as an internal standard for quantification. Additional experimental details are reported in ref. 45.

Liquid chromatography–tandem mass spectrometry. Liquid chromatography–tandem mass spectrometry analyses were carried out with an Agilent 1200 HPLC interfaced to a TSQ Quantum Ultra triple-stage quadrupole mass spectrometer (Thermo-Finnigan, San Jose, CA). An HSF5 column (4.5 × 150 mm, 5 μm, Supelco) was used for LC separation. The internal standards (NNN-d_4 and NNK-d_4, 10 μL of 1 $\mu g\,mL^{-1}$) and 0.5 mL of 1 M H_2SO_4 were added to 100-μL aliquots of the methanol extracts. The solutions were washed with 4 mL of 1:2 (vol/vol) toluene/ethyl acetate. The aqueous phases were made basic with 0.5 mL of 50% aqueous potassium carbonate and then extracted with 4 mL of 1:2 toluene/ethyl acetate. The extracts were evaporated by using a centrifugal vacuum evaporator, reconstituted in 150 μL of 10% methanol in 12 mM aqueous HCl, and chromatographed with a methanol and water solvent system containing 10 mM ammonium formate at 0.9 mL/ min by using a linear gradient from 25% to 100% methanolic buffer. Atmospheric pressure chemical ionization was used. The mass spectrometer was operated in the selected reaction monitoring mode. The transitions 178 to 148 and 182 to 152 at a collision energy of 8 eV were used for NNN and the internal standard, NNN-d_4, respectively. The transitions 208 to 122 and 212 to

126 at a collision energy of 12 eV were used for NNK and the internal standard, NNK-d_4, respectively.

ACKNOWLEDGMENTS. We express our gratitude to S. Schick (University of California San Francisco), C.J. Weschler (Environmental & Occupational Health Science Institute, Rutgers University, and Technical University of Denmark), K. Asotra (University of California Tobacco-Related Diseases Research Program), and W.J. Fisk (LBNL) for helpful suggestions and to R. Maddalena, M. Russell, R. Dod, F. Mizbani, E. Smith (LBNL), W. Luo, C. Chen, W. Ascher (Portland State University), C. Havel, and M. Goniewicz (University of California San Francisco) for their assistance. We also thank the journal editor and reviewers for their helpful suggestions. This work was supported by the University of California Tobacco-Related Diseases Research Program (Project 16RT-0158). Experimental work was carried out at LBNL under US Department of Energy Contract DE-AC02-05CH11231. Laboratory resources at University of California San Francisco were supported by the Flight Attendant Medical Research Institute and by National Institutes of Health Grant DA012393.

1. International Agency for Research on Cancer (2004) *Tobacco Smoke and Involuntary Smoking*, IARC Monographs (International Agency for Research on Cancer, Lyon, France), Vol 83.
2. US Department of Health and Human Services (2006) *The Health Consequences of Involuntary Exposure to Tobacco Smoke: A Report of the Surgeon General* (Center for Disease Control and Prevention, Atlanta, GA) http://www.surgeongeneral.com/library/secondhandsmoke/report/.
3. Matt GE, et al. (2004) Households contaminated by environmental tobacco smoke: Sources of infant exposures. *Tob Control* 13:29–37.
4. Winickoff J, et al. (2009) Beliefs about the health effect of "thirdhand" smoke and home smoking bans. *Pediatrics* 123:E74–E79.
5. Daisey JM (1999) Tracers for assessing exposure to environmental tobacco smoke: What are they tracing?. *Environ Health Persp* 107:319–327.
6. Singer BC, Hodgson AT, Nazaroff WW (2003) Gas-phase organics in environmental tobacco smoke: 2. Exposure-relevant emission factors and indirect exposure from habitual smoking. *Atmos Environ* 37:5551–5561.
7. Singer BC, Revzan KL, Hotchi T, Hodgson AT, Brown NJ (2004) Sorption of organic gases in a furnished room. *Atmos Environ* 38:2483–2494.
8. Destaillats H, Singer BC, Lee SK, Gundel LA (2006) The effect of ozone on nicotine desorption from model surfaces: Evidence for heterogeneous chemistry. *Environ Sci Technol* 40:1799–1805.
9. Hecht SS (2003) Tobacco carcinogens, their biomarkers and tobacco-induced cancer. *Nat Rev Cancer* 3:733–744.
10. Pankow JF, Watanabe KH, Toccalino PL, Luo W, Austin DF (2007) Calculated cancer risks for conventional and "potentially reduced exposure product" cigarettes. *Cancer Epidem Biomar* 16:584–592.
11. Finlayson-Pitts BJ, Pitts JN (2000) *Chemistry of the Upper and Lower Atmosphere* (Academic, San Diego, CA).
12. Wainman T, Weschler CJ, Lioy P, Zhang J (2001) Effects of surface type and relative humidity on the production and concentration of nitrous acid in a model indoor environment. *Environ Sci Technol* 35:2200–2206.
13. Lee K, et al. (2002) Nitrous acid, nitrogen dioxide and ozone concentrations in residential environments. *Environ Health Persp* 110:145–149.
14. Spengler JD, Brauer M, Samet JM, Lambert WE (1993) Nitrous acid in Albuquerque, New Mexico, homes. *Environ Sci Technol* 27:841–845.
15. Pitts JN, et al. (1989) Time-resolved identification and measurement of indoor air pollutants by spectroscopic techniques: Gaseous nitrous acid, methanol, formaldehyde and formic acid. *JAPCA J Air Waste Ma* 39:1344–1347.
16. Eatough DJ, et al. (1989) Chemical composition of environmental tobacco smoke. 1. Gas-phase acids and bases. *Environ Sci Technol* 23:679–687.
17. Goodman AL, Underwood GM, Grassian VH (1999) Heterogeneous reaction of NO_2: characterization of gas-phase and adsorbed products from the reaction, $2NO_2(g) + H_2O(a) - HONO(g) + HNO_3(a)$ on hydrated silica particles. *J Phys Chem A* 103:7217–7223.
18. Finlayson-Pitts BJ, Wingen LM, Sumner AL, Syomin D, Ramazan KA (2003) The heterogeneous hydrolysis of NO_2 in laboratory systems and in outdoor and indoor atmospheres: An integrated mechanism. *Phys Chem Chem Phys* 5:223–242.
19. Mertes S, Wahner A (1995) Uptake of nitrogen dioxide and nitrous acid on aqueous surface. *J Phys Chem* 99:14000–14006.
20. Hirokawa J, Kato T, Mafun F (2008) Uptake of gas-phase nitrous acid by pH-controlled aqueous solution studied by a wetted wall flow tube. *J Phys Chem A* 112:12143–12150.
21. Yabushita A, et al. (2009) Anion-catalyzed dissolution of NO_2 on aqueous microdroplets. *J Phys Chem A* 113:4844–4848.
22. Enami S, Hoffmann MR, Colussi AJ (2009) Absorption of inhaled NO_2. *J Phys Chem B* 113:7977–7981.
23. Febo A, Perrino C (1995) Measurement of high concentration of nitrous acid inside automobiles. *Atmos Environ* 29:345–351.
24. Pitts JN, Grosjean D, Van Cauwenberghe K, Schmid JP, Fitz DR (1978) Photooxidation of aliphatic amines under simulated atmospheric conditions: Formation of nitrosamines, nitramines, amides and photochemical oxidant. *Environ Sci Technol* 12:946–953.
25. Hecht SS, et al. (1978) Chemical studies on tobacco smoke. 52. Reaction of nicotine and sodium nitrite: formation of nitrosamines and fragmentation of the pyrrolidine ring. *J Org Chem* 43:72–76.
26. Morrison GC, Zhao P, Kasthuri L (2006) The spatial distribution of pollutant transport to and from indoor surfaces. *Atmos Environ* 40:3677–3685.
27. Cano-Ruiz JA, Kong D, Balas R, Nazaroff WW (1993) Removal of reactive gases at indoor surfaces: Combining mass transport and surface kinetics. *Atmos Environ* 27A:2039–2050.
28. Peterson LA, Castagnoli N (1988) Regio- and stereochemical studies on the α-carbon oxidation of (S)-nicotine by cytochrome P-450 model system. *J Med Chem* 31:637–640.
29. Strlic M, Cigic IK, Kolar J, de Bruin G, Pihlar B (2007) Non-destructive evaluation of historical paper based on pH estimation from VOC emissions. *Sensors* 7:3136–3145.
30. Hecht SS, Chen C-HB, Hoffmann D (1979) Tobacco-specific nitrosamines: Occurrence, formation, carcinogenicity and metabolism. *Acc Chem Res* 12:92–98.
31. Kobayashi SA, Sakata H, Mitsu K, Tanoue H (2007) A possible photosensitizer: Tobacco-specific nitrosamine, 4-(N-methylnitrosamino)-1-(3-pyridyl)-1-butanone (NNK), induced mutations, DNA strand breaks and oxidative and methylative damage with UVA. *Mutat Res* 632:111–120.
32. Crespi CL, Penman BW, Gelboin HV, Gonzalez FJ (1991) A tobacco smoke-derived nitrosamine, 4-(methylnitrosamino)-1-(3-pyridyl)-1-butanone, is activated by multiple human cytochrome P450s including the polymorphic human cytochrome P4502D6. *Carcinogenesis* 12:1197–1201.
33. Jacob P, III, et al. (2008) Subpicogram per milliliter determination of the tobacco-specific carcinogen metabolite 4-(methylnitrosamino)-1-(3-pyridyl)-1-butanol in human urine using liquid chromatography-tandem mass spectrometry. *Anal Chem* 80:8115–8121.
34. Hecht SS, Tricker AR (1999) *Analytical Determination of Nicotine and Related Compounds and Their Metabolites*, ed Gorod JW (Elsevier, Amsterdam), pp 421–488.
35. Hoffmann D, Brunnemann KD, Prokopczyk B, Djordjevic MV (1994) Tobacco-specific N-nitrosamines and areca-derived N-nitrosamines: Chemistry, biochemistry, carcinogenicity and relevance to humans. *J Toxicol Environ Health* 41:1–52.
36. Pankow JF, Asher WE (2008) SIMPOL 1: A simple group contribution method for predicting vapor pressures and enthalpies of vaporization of multifunctional organic compounds. *Atmos Chem Phys* 8:2773–2796.
37. Weschler CJ, Nazaroff WW (2008) Semivolatile organic compounds in indoor environments. *Atmos Environ* 42:9018–9040.
38. Matt GE, et al. (2008) Residual tobacco smoke pollution in used cars for sale: Air, dust and surfaces. *Nicotine Tob Res* 10:1467–1475.
39. Wisthaler A, Weschler CJ (2009) Reactions of ozone with human skin lipids: Sources of carbonyls, dicarbonyls, and hydroxycarbonyls in indoor air. *Proc Natl Acad Sci USA* doi:10.1073/pnas.0904498106.
40. Corsi RL, Siegel J, Karamalegos A, Simon H, Morrison GC (2007) Personal reactive clouds: Introducing the concept of near-head chemistry. *Atmos Environ* 41:3161–3165.
41. Rim D, Novoselec A, Morrison GC (2009) The influence of chemical interactions at the human surface on breathing zone levels of reactants and products. *Indoor Air* 19:324–334.
42. Schick SF, Glantz S (2007) Concentrations of the carcinogen 4-(methylnitrosamino)1-(3-pyridyl)-1-butanone in sidestream cigarette smoke increase after release into indoor air: results from unpublished tobacco industry research. *Cancer Epidem Biomar* 16:1547–1553.
43. Raff JD, et al. (2009) Chlorine activation indoors and outdoors via surface-mediated reactions of nitrogen oxides with hydrogen chloride. *Proc Natl Acad Sci USA* 106:13647–13654.
44. Taira M, Kanda Y (1990) Continuous generation system for low-concentration gaseous nitrous acid. *Anal Chem* 62:630–633.
45. Sleiman M, Maddalena RL, Gundel LA, Destaillats H (2009) Rapid and sensitive gas chromatography ion-trap mass spectrometry method for the determination of tobacco-specific N-nitrosamines in secondhand smoke. *J Chromatogr A* 1216:7899–7905.